



Contents lists available at ScienceDirect

Arabian Journal of Chemistry

journal homepage: www.ksu.edu.sa

Original article

Quantitative analysis of active components in *Rhodiola* species based on disease module-guided network pharmacologyJian Zhu^a, Ruyi Jin^a, Mei Su^b, Jierong Pei^c, Yanxu Chang^b, Miaomiao Jiang^{a,*}^a State Key Laboratory of Component-based Chinese Medicine, Tianjin University of Traditional Chinese Medicine, 10 Poyanghu Road, Jinghai District, Tianjin 301617, China^b Haihe Laboratory of Modern Chinese Medicine, Tianjin 301617, China^c Tianjin Key Laboratory of Therapeutic Substance of Traditional Chinese Medicine, Tianjin 301617, China

ARTICLE INFO

Keywords:

Rhodiola species
Chemical profile
Network pharmacology
Quantitative analysis
Quality markers

ABSTRACT

Many different species of *Rhodiola* are traditional botanical medicines with various effects, and their roots and rhizomes are the medicinal parts, which have been recorded in many ancient medical books. The 2020th edition of Chinese Pharmacopoeia stipulates *Rhodiola crenulata* (Hook. f. et Thoms.) H. Ohba (*R. crenulata*) as the only medicinal species. However, the wild resources of *R. crenulata* are gradually decreasing, and it is difficult to achieve artificial cultivation of *R. crenulata* nowadays. It is important to find several alternative species of *R. crenulata*. In the present study, an integrated strategy based on chemical profiling, disease module-guided network pharmacology, and quantitative analysis (CDMQ) has been developed to estimate the chemical characteristics, determine active components and related disease modules, discover potential quality markers, and identify alternative species in a step-by-step manner for 9 species of *Rhodiola*. Firstly, a total of 109 compounds were identified in accordance with their retention times, accurate masses and characteristic MS/MS fragment patterns, which mainly included phenylpropanoid glycosides, gallic acid glycosides, flavonoids and their glycosides, flavanols, organic acids, and others. Subsequently, disease module-guided network pharmacology analysis was performed based on the related targets of 109 compounds. In combination of the limit of detection of the UPLC-QQQ-MS/MS, 12 compounds were identified as active components. The enriched disease modules of circulatory system, mouth, respiratory system, skin and connective tissue showed close relationship with traditional efficacy of *Rhodiola* species. It also revealed that salidroside, rhodiosin, epicatechin gallate, catechin gallate, and 6'-*O*-galloylsalidroside changed significantly in different species to be served as potential quality markers for *Rhodiola*. Among the 9 species, *Rhodiola kirilowii* (Regel) Maxim (*R. kirilowii*) and *Rhodiola sacra* (Prain ex Hamet) S.H. Fu (*R. sacra*) could probably be used as an alternative species of *R. crenulata*. Overall, this study established a solid foundation and provided theoretical guidance for the chemical profiling, prediction of clinical application, and quality control of different *Rhodiola* species.

1. Introduction

The genus *Rhodiola* belongs to the family Crassulaceae and grows in high-altitude and other cold areas of the northern hemisphere. It has been widely used in both Asia and Europe. There are 96 species of *Rhodiola* in the world, with the majority being found in different regions of China, and 73 species of *Rhodiola* mainly distribute in Qinghai, Tibetan, Sichuan, and Yunnan provinces. Despite abundant species in *Rhodiola* genus, only limited species have been extensively investigated so far (Zhuang et al., 2019; Tao et al., 2019; Shikov et al., 2021; Panossian et al., 2021).

Several species in *Rhodiola* genus as herbal medicine have been mentioned in ancient medicine, such as "Four Medical Tantras", "Shennong's Classic of Materia Medica", "Compendium of Materia Medica", and "Jing-Zhu Materia Medica", which include *Rhodiola crenulata* (Hook. f. et Thoms.) H. Ohba (*R. crenulata*), *Rhodiola kirilowii* (Regel) Maxim (*R. kirilowii*), *Rhodiola sacra* (Prain ex Hamet) S.H. Fu (*R. sacra*), *Rhodiola himalensis* (D. Don) S.H. Fu (*R. himalensis*), *Rhodiola wallichiana* (Hook.) S.H. Fu (*R. wallichiana*), *Rhodiola wallichiana* var. *cholaensis* (Praeger) S.H. Fu (*R. wallichiana* var.), *Rhodiola tieghemii* (Raym.-Hamet) S.H. Fu (*R. tieghemii*), *Rhodiola fastigiata* (Hook. f. & Thomson) S.H. Fu (*R. fastigiata*), and *Rhodiola yunnanensis* (Franch.) S.H.

* Corresponding author.

E-mail address: miaomiaojiang@tjutcm.edu.cn (M. Jiang).<https://doi.org/10.1016/j.arabjc.2023.105570>

Received 21 August 2023; Accepted 14 December 2023

Available online 20 December 2023

1878-5352/© 2023 The Author(s). Published by Elsevier B.V. on behalf of King Saud University. This is an open access article under the CC BY-NC-ND license (<http://creativecommons.org/licenses/by-nc-nd/4.0/>).

Fu (*R. yunnanensis*). According to the basic tenets of Traditional Chinese Medicine (TCM), roots and rhizomes of *Rhodiola* can boost qi and dissipate blood stasis, unblock the blood vessels, relieve pain, fortify the spleen, treat heart palpitations, ease coughing and shortness of breath, and reduce fatigue and weakness. Due to various medicinal virtues, the demand for *Rhodiola* plant increases, and the wild resources of *R. crenulata* have rapidly declined, which has been recognized as a medicinal origin in Chinese Pharmacopoeia (Chinese Pharmacopoeia Commission, 2020; Wang et al., 2023; Teng et al., 2022). Furthermore, cultivating *R. crenulata* artificially has been proven to be challenging (Wen et al., 2016; Zhao et al., 2018; Zhong et al., 2022).

Current pharmacological investigations have revealed that these *Rhodiola* species exhibit therapeutic value for many diseases such as Alzheimer's disease (AD) (Zhang et al., 2016; Diermen et al., 2009), lung diseases (Hsu et al., 2017; Jia et al., 2023), cerebrovascular disease (Ma

et al., 2017), diabetes (Jafari et al., 2022; Zheng et al., 2019), cardiovascular disease (CVD) (Chen et al., 2022a; Liu et al., 2016), and aging-related diseases (Liang et al., 2023). For example, the 70% ethanol extract of *R. crenulata* showed superior regulatory effects on senescence, as demonstrated by senescence-associated β -galactosidase (SA β G) staining assays and lifespan analysis. The 50% ethanol extract of *R. kirilowii* was confirmed to possess potent immunomodulatory activity (Wojcik et al., 2009). The extract of *R. sacra* has been demonstrated with strong efficacy on mitigating histological changes in lung tissue and alleviating inflammatory stimulation induced by lipopolysaccharide (LPS) (Jung et al., 2008). Additionally, compounds in *Rhodiola* extracts including salidroside, epicatechin gallate, catechin gallate, rhodiosin, luteolin, epicatechin, catechin, and afzelin were considered to be the major contributors of the observed bioactivities (Chu et al., 2014; Döring et al., 2022; Grosso et al., 2023; Choe et al., 2012; Wang et al.,

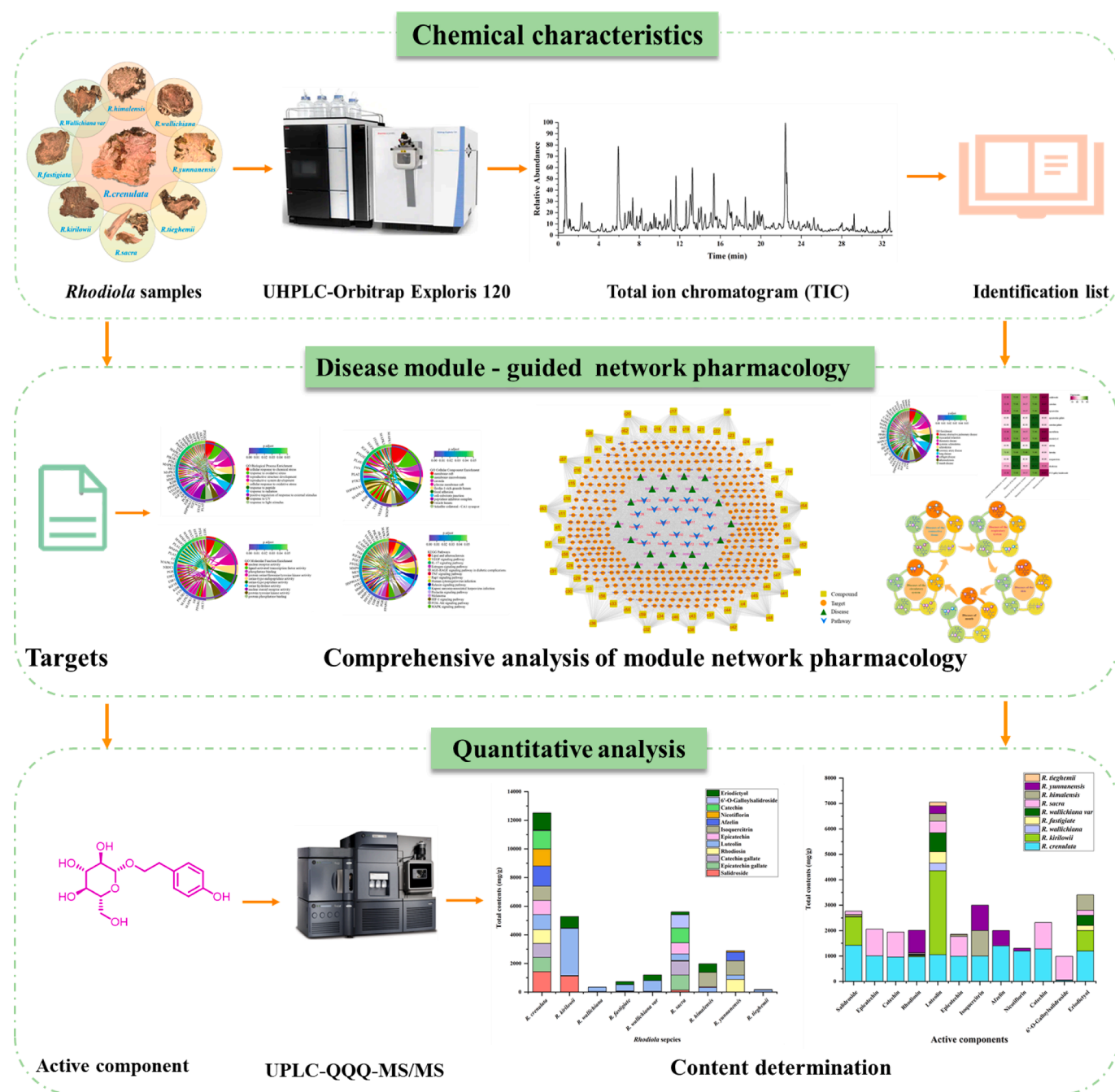


Fig. 1. Summary diagram of the established chemical profiling, disease module-guided network pharmacology and quantitative analysis (CDMQ) strategy.

2023).

Network pharmacology is an emerging field that utilizes high-throughput omics data analysis and computer-based algorithms to understand the complex interactions within biological systems (Li and Zhang, 2013; Sun et al., 2022a; Hopkins, 2007). It involves the use of computational tools and network databases for analyzing and retrieving information related to biological networks. Network pharmacology can be utilized to construct modules that forecast relationships between compounds and targets. (Park et al., 2018; Ye et al., 2020). Due to the characteristics of “multi-component, multi-target, and multi-pathway”, traditional Chinese medicine possess a wealth of pharmacological activities and are widely utilized in the treatment of various diseases (Parham et al., 2020). However, network pharmacology studies commonly focus on specific disease, which limits the exploration of various therapeutic effects of traditional Chinese medicine. When dealing with herbs or plants characterized by unidentified pharmacological activities, the ailments for which they can provide therapeutic benefits remained uncharted territory. Consequently, the conventional approach to network pharmacology research becomes inadequate in such instances.

An integrated strategy based on chemical profiling, disease module-guided network pharmacology, and quantitative analysis (CDMQ) was developed in the present study (Fig. 1). The UHPLC-Orbitrap Exploris MS analysis method was established for the global characterization of chemical composition of *Rhodiola* species. Moreover, the disease module-guided network pharmacology was performed to identify active components with various pharmacological actions. Finally, in combination with quantitative analysis, a series of potential quality markers that regulated each disease module were identified for different *Rhodiola* species. Meanwhile, alternative species of *R. crenulata* were elucidated based on quality markers. The CDMQ analysis method was conducted to establish a solid chemical foundation for disease module-guided network pharmacology and provide theoretical guidance for the evaluation of different *Rhodiola* species to evaluate alternative species for *R. crenulata*.

2. Materials and methods

2.1. Materials and reagents

Mature roots and rhizomes of 9 *Rhodiola* species, namely *R. crenulata*, *R. kirilowii*, *R. wallichiana*, *R. fastigiata*, *R. wallichiana* var., *R. sacra*, *R. himalensis*, *R. yunnanensis*, *R. tieghemii*, which were collected from Yunnan Province and Tibet Autonomous Region (Table S1). All samples were authenticated by Dr. Honghua Wu (Tianjin University of Traditional Chinese Medicine). The specimens (voucher number RC20200627 for *R. crenulata*, number RK20200623 for *R. kirilowii*, number RW20200624 for *R. wallichiana*, number RF20200624 for *R. fastigiata*, number RWV20200909 for *R. wallichiana* var., number RS20200802 for *R. sacra*, number RH20200921 for *R. himalensis*, number RY20201122 for *R. yunnanensis* and number RT20210726 for *R. tieghemii*) were stored at the State Key Laboratory of Component-based Chinese Medicine.

Formic acid (MS grade) was acquired from ACS business in the United States, acetonitrile and methanol (chromatographic purity) were obtained from Fisher company in the United States, and ultrapure water was sourced from Guangzhou Watsons Food and Beverage Company in Guangzhou, China. The reference compounds of herbacetin, catechin gallate, 6'-O-galloylsalidroside, rosavin, eriodictyol, afzelin, kaempferol-3-O-rutinoside, 3,4,5-trimethoxycinnamic acid, rhodiosin, and crenulatin were obtained from Sichuan Weikeqi Biotech Co., Ltd. in Chengdu, China. Citric acid, epicatechin gallate, gallic acid, catechin, epicatechin, caffeic acid, salidroside, quercetin, luteolin, kaempferol, isocitricin, and quercitrin were acquired from Shanghai Yuanye Bio-Technology Co., Ltd. in Shanghai, China.

2.2. Preparation of *Rhodiola* extracts and UHPLC-orbitrap exploris MS analysis

The samples of *Rhodiola* species were crushed into powder and stored in a desiccator. The finely ground powder (100 mg) was accurately weighed and ultrasonically extracted with 10 mL of 70% methanol (v/v) at room temperature for 30 min (Dong et al., 2023). After extraction, 70% methanol (v/v) was added to compensate for the weight loss. The extract was centrifuged at 14,000 rpm for 10 min. The supernatant was collected and dried, then redissolved in 1 mL methanol. In order to remove non-polar components and improve solubility, samples were eluted with methanol using an SPE column. The eluate was then dried and redissolved in methanol before being filtered through 0.22 μ m membrane for further UHPLC-Orbitrap Exploris MS analysis. One milligram of each reference standard was accurately weighed and dissolved in 1 mL of methanol. After mixing with 22 reference standard solutions, a mixed and diluted sample was obtained with a concentration of 200 ng/mL for each standard.

The UHPLC separation was performed on a Vanquish UHPLC System (Thermo Fisher Scientific, San Jose, CA, USA) with a Waters ACQUITY HSS T3 column (2.1 \times 100 mm, 1.8 μ m) maintained at 40 $^{\circ}$ C, using a binary mobile phase consisting of 0.1% FA in water (A) and acetonitrile (B) (Ma et al., 2022). The mobile phase flow rate was set at 0.4 mL/min using an optimal gradient elution program, which consisted of the following: 0–8 min 3%–13% (B), 8–25 min 13%–30% (B), 25–30 min 30%–45% (B), and 30–33 min 45%–95% (B). The injection volume was set to 2 μ L. High-resolution MS data were collected in both positive and negative modes using the UHPLC-Orbitrap Exploris 120 coupled with an Orbitrap Mass Spectrometer. The source parameters were set as follows: spray voltage, -3.5 kV/+3.5 kV; Ion Transfer Tube Temp, 320 $^{\circ}$ C; Vaporizer Temp, 350 $^{\circ}$ C; Normalized collision energy, 20/40/60 V; Sheath gas (N₂), 35 arb; Auxiliary gas (N₂), 10 arb; Sweep gas (N₂), 0 arb. The scanning method of Full MS/dd-MS2 (TopN) was used to acquire data. The full scan range of MS¹ was 100–1500 m/z with a resolution of 120,000, and MS² scan range was 100–1500 m/z with a resolution of 15,000. The Xcalibur™ 4.1 software was used for data acquisition and processing.

2.3. Disease module-guided network pharmacology

Three databases were searched to identify the targets of chemical components in *Rhodiola* species as presented in Table S2. The databases searched included Swiss Target Prediction (<https://www.swisstargetprediction.ch/>) (Ge et al., 2019), ChEMBL (<https://www.ebi.ac.uk/chembl/>) (Mendez et al., 2019), and ETCM (<https://www.tcmip.cn/ETCM/>) (Xu et al., 2018). The targets were converted into gene symbols using Uniprot (<https://www.uniprot.org/>) (Coudert et al., 2023), and the gene symbols were then combined.

The R language Bioconductor package was utilized to conduct Gene Ontology (GO), Kyoto Encyclopedia of Genes and Genomes (KEGG) pathway, and Disease Ontology (DO) enrichment analysis. The cut-off criterion for significant GO, pathway, and disease terms was set at a p -value < 0.01. The top enriched terms were visualized using an online tool (<https://sangerbox.com/home.html>) (Shen et al., 2022).

The compound-target-pathway-disease network was constructed using Cytoscape 3.8.2. In this network, nodes represented compounds, core targets, core pathways, and core diseases, while edges denoted the interactions among them. The number of direct connections between one node and any other nodes in the network was known as the node degree.

Based on the results of disease ontology enrichment analysis, the top 10 diseases were selected. Following the 11th revision of the International Classification of Diseases (ICD-11) issued by the World Health Organization, the top 10 diseases were grouped into five disease modules. The intersection between the related targets of each disease module and the targets of 12 active components was determined. Subsequently,

the proportion of the intersection targets corresponding to each active component in the related targets of each disease module was calculated. Finally, the active component that corresponded to each disease module was selected to construct the disease module-active component network.

2.4. Preparation of *Rhodiola* extracts and UPLC-QQQ-MS/MS analysis

Nine *Rhodiola* samples were crushed into a powder and stored in a desiccator until extraction. To extract, 100 mg of the finely ground powder was accurately weighed and ultrasonically treated in 10 mL of 70% methanol (v/v) for 30 min at room temperature. After extraction, 70% methanol (v/v) was added to compensate for any weight loss. For additional analysis using UPLC-QQQ-MS/MS, the extract's supernatant was filtered through 0.22 μ m membrane following centrifugation at 14,000 rpm for 10 min. The following gradient elution was used to carry out the chromatographic analysis on an ACQUITY UPLC Ultra Performance Liquid Chromatograph (American, Waters Company), the Fortis C18 (2.1 \times 100 mm, 1.7 μ m) was kept at 40 $^{\circ}$ C. The mobile phase was composed of 0.1% formic acid solution (A) and acetonitrile (B). The flow rate was set at 0.3 mL/min, and the time intervals were as follows: 0–2 min 2% B, 2–2.1 min 2–57% B, 2.1–4.5 min 64–95% B, and 4.6–6 min 95–98% B. Waters Xevo TQ-S Triple Quadrupole Mass Spectrometer (American, Waters company) was used for MS detection. The multiple reaction monitoring (MRM) method was used to quantify the active components (Ren et al., 2022). The ion source was an electrospray ionization (ESI). The operating parameters were optimized as follows:

desolvation temperature 350 $^{\circ}$ C; cone voltage 37 V; capillary voltage 2.0 KV (Liu et al., 2024). An overview of the 12 compounds and their mass spectrometry analysis conditions are provided in Table S4 and Table S5.

2.5. Method validation of quantitative analysis

The limit of detection (LOD), limit of quantification (LOQ), precision, repeatability, stability, and accuracy of the 12 active components were determined using “2.4” extraction procedures and analytical conditions. The standard curve was constructed with the concentration (x, ng/mL) of the reference substance as the abscissa and the corresponding peak area (y) of each reference substance as the ordinate. Linear regression was then performed on the standard curve to examine the correlation coefficient and linear range of the resulting equation. The concentration of each component was considered as the LOD or LOQ when the signal-to-noise ratio (S/N) was 3 or 10, respectively. Intra- and inter-day precisions were calculated by conducting repeated analysis on the same day (intra-day precision) and three days apart (inter-day precision). The stability of the samples was observed after being kept at room temperature for 0, 2, 4, 8, 12, and 24 h. The accuracy of the method was validated through recovery experiments performed using the standard addition method.

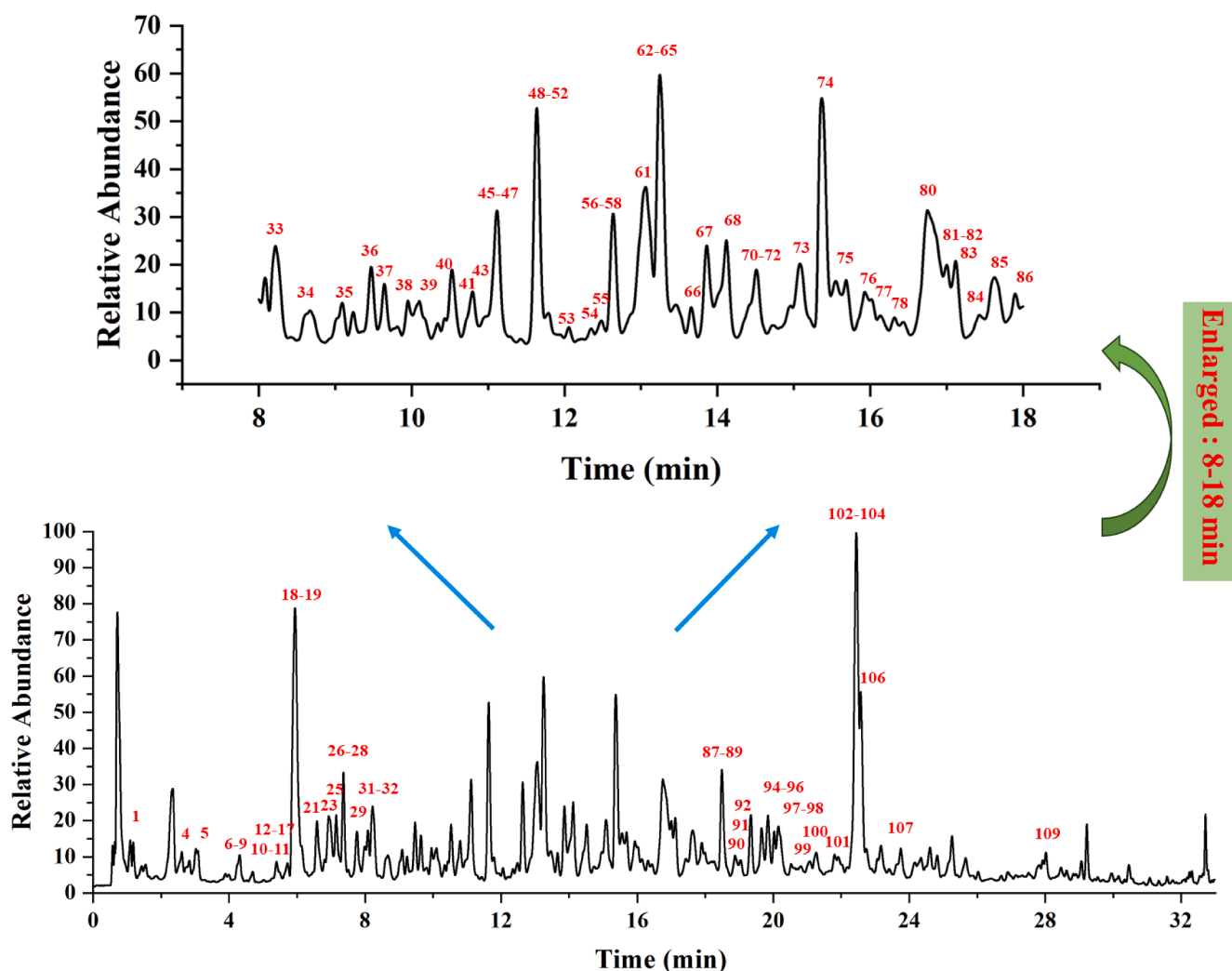


Fig. 2. The total ion chromatogram (TIC) of the *R. crenulata* extract by UHPLC-Orbitrap Exploris 120 MS analysis.

3. Result

3.1. Identification of compounds in the extracts of *Rhodiola species*

The total ion chromatogram of the extract of *R. crenulata* is displayed in Fig. 2 and a total of 109 compounds are elucidated, including 10 phenylethanoid glycosides, 20 gallic acid glycosides, 19 flavonoids and their glycosides, 18 flavanols, 11 organic acids, 6 lignans, 5 acyclic alcohol glycosides and others. Twenty compounds were unquestionably assigned by comparing them with the corresponding reference compounds and 89 compounds were tentatively recognized by comparing the empirical molecular formulas and mass fragments with those of the known constituents mentioned in the literature. In addition, 93 compounds were identified in *R. crenulata*, 16 compounds were identified in *R. tieghemii*, 25 compounds were identified in *R. wallichiana*, 31 compounds were identified in *R. fastigiata*, 49 compounds were identified in *R. sacra*, 24 compounds were identified in *R. wallichiana var.*, 41 compounds were identified in *R. yunnanensis*, 39 compounds were identified in *R. himalensis*, and 33 compounds were identified in *R. kirilowii*. The identification and distribution lists for the compounds in 9 species of *Rhodiola* are shown in Table S2 and Table S3.

3.2. Active components elucidated by disease module-guided network pharmacology analysis

3.2.1. Enrichment analysis of compound-related targets of *Rhodiola species*

After removing duplicate values, the total number of relevant predicted targets for the 109 compounds was 357. The targets of 109 compounds were submitted to the Bioconductor package of the R language for GO, KEGG pathway, DO enrichment analysis. The GO enrichment analysis results showed that 1997 GO terms were enriched, including 1810 biological processes, 60 cellular components, and 127 molecular functions. The top 10 significantly enriched terms were extracted from the three categories according to the $p.adjust$ ($p < 0.01$) and displayed by chord diagrams in Fig. 3A–C. The KEGG enrichment

analysis showed the involvement of 135 pathways with p -adjustments smaller than 0.01. The top 15 signaling pathways are displayed in Fig. 3D, including lipid and atherosclerosis, VEGF signaling pathway, IL-17 signaling pathway, estrogen signaling pathway, among others. The DO enrichment analysis indicated the involvement of 445 diseases with an adjusted p -value of less than 0.01. To avoid the influence of cancer and tumor diseases, related disorders were excluded from the prediction results due to the prevalence of targets associated with these diseases. The top 10 diseases are illustrated in a chord diagram and are presented in Fig. 4A, including chronic obstructive pulmonary disease, myocardial infarction, rheumatic disease, systemic scleroderma, scleroderma, coronary artery disease, lung disease, collagen disease, atherosclerosis, and mouth diseases.

3.2.2. Compound-target-pathway-disease network analysis

The candidate compounds, their corresponding targets, core pathways, and associated diseases were analyzed using Cytoscape 3.8.2 for network visualization. The top 20 pathways and diseases were selected, while broad-spectrum pathways and diseases, such as those related to cancer and proteoglycans in cancer were excluded, as depicted in Fig. 5. The resulting network graph, which consists of 470 nodes and 6858 edges, indicates the presence of complex correlations among different compounds, targets, pathways, and diseases. Active components were determined based on a degree ≥ 150 for these components, such as 6'-*O*-galloylsalidroside (c26, degree = 211) and salidroside (c7, degree = 198). A total of 12 components were considered as active components, which were shown in Table S4.

3.2.3. Disease module-guided network pharmacology analysis

According to the International Classification of Diseases 11th Revision (ICD-11), the concept of disease module was introduced. The top 10 diseases were divided into five disease modules. Chronic obstructive pulmonary disease and lung disease were integrated into the disease module of the respiratory system. Myocardial infarction, coronary artery disease and atherosclerosis were integrated into the disease module of

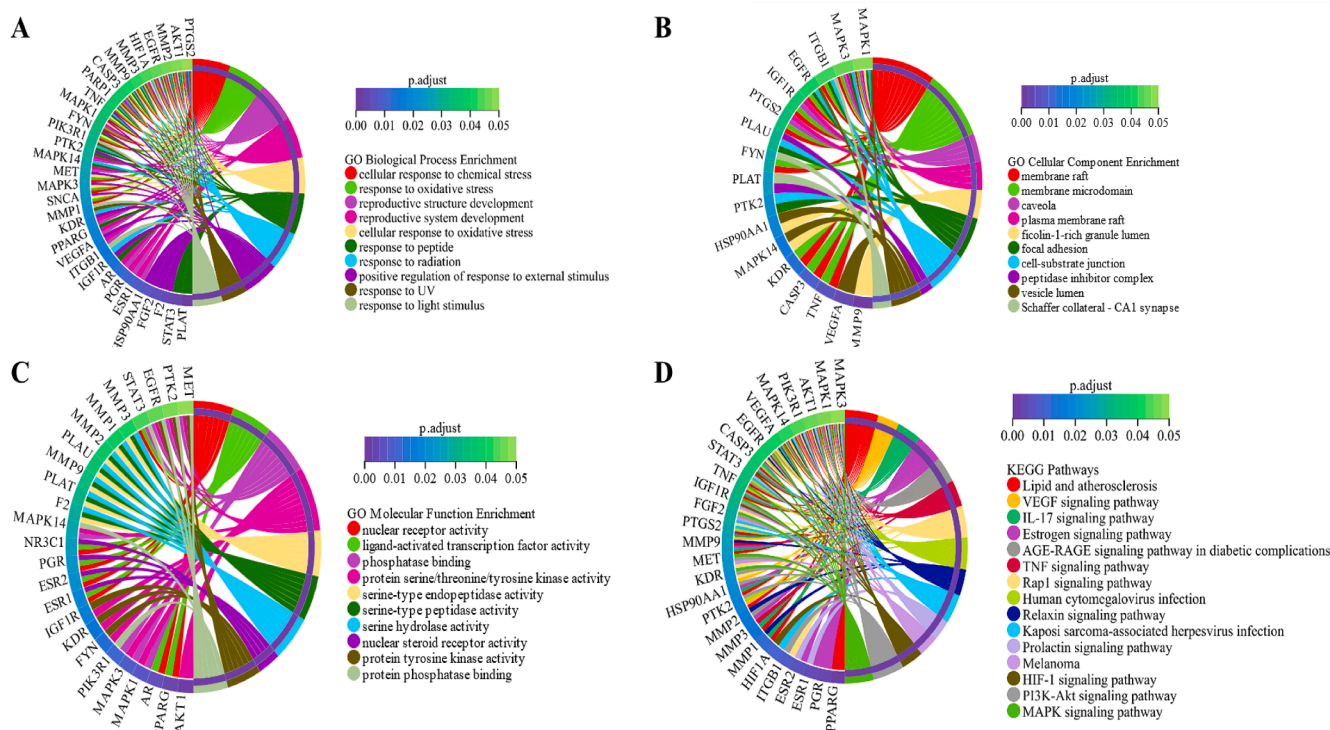


Fig. 3. Gene ontology (GO) enrichment and Kyoto Encyclopedia of Genes and Genomes (KEGG) pathway analysis of the targets of 109 compounds in *Rhodiola* species. A: Biological Process; B: Cellular Component; C: Molecular Function; D: KEGG pathway.

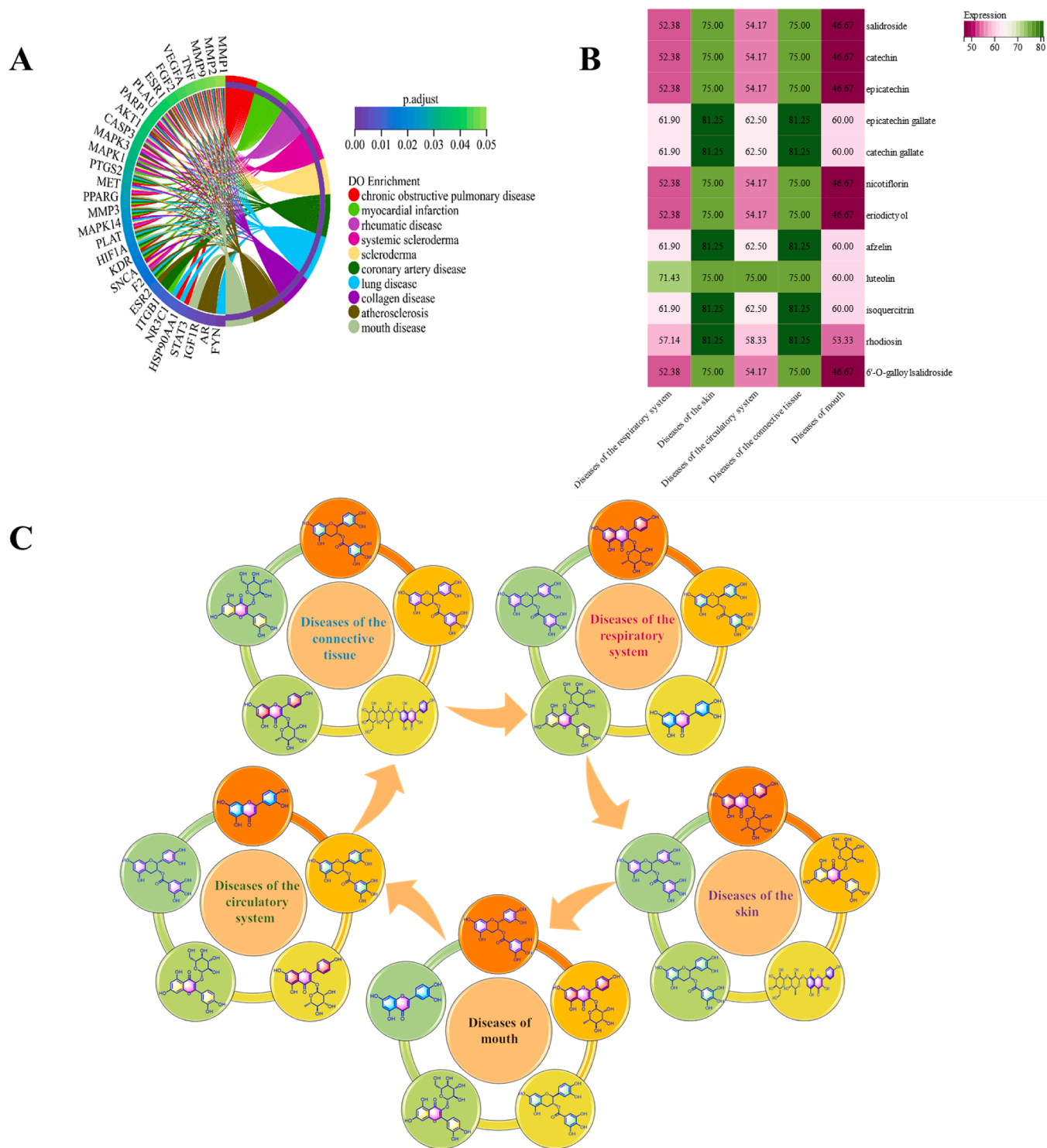


Fig. 4. Selection of active compounds based on disease module-guided network pharmacology analysis. A: The Disease Ontology (DO) enrichment analysis, B: The heatmap between active compounds and five disease modules, C: the disease module – active component network.

the circulatory system. Systemic sclerosis and scleroderma were integrated into the disease module of the skin. Rheumatic diseases and collagen diseases were integrated into the disease module of the connective tissue, and mouth disease was summarized into the disease module of the mouth. Subsequently, by means of the proportion of intersection targets corresponding to each active component in the related targets of each disease module (Fig. 4B), disease module-active component network diagram was constructed (Fig. 4C). In the disease

modules of the circulatory system, the respiratory system, and the mouth, luteolin, epicatechin gallate, catechin gallate, afzelin, and isoquercitrin played crucial roles. In the disease modules of the skin and the connective tissue, the active components that played significant roles were epicatechin gallate, catechin gallate, afzelin, isoquercitrin, and rhodiosin.

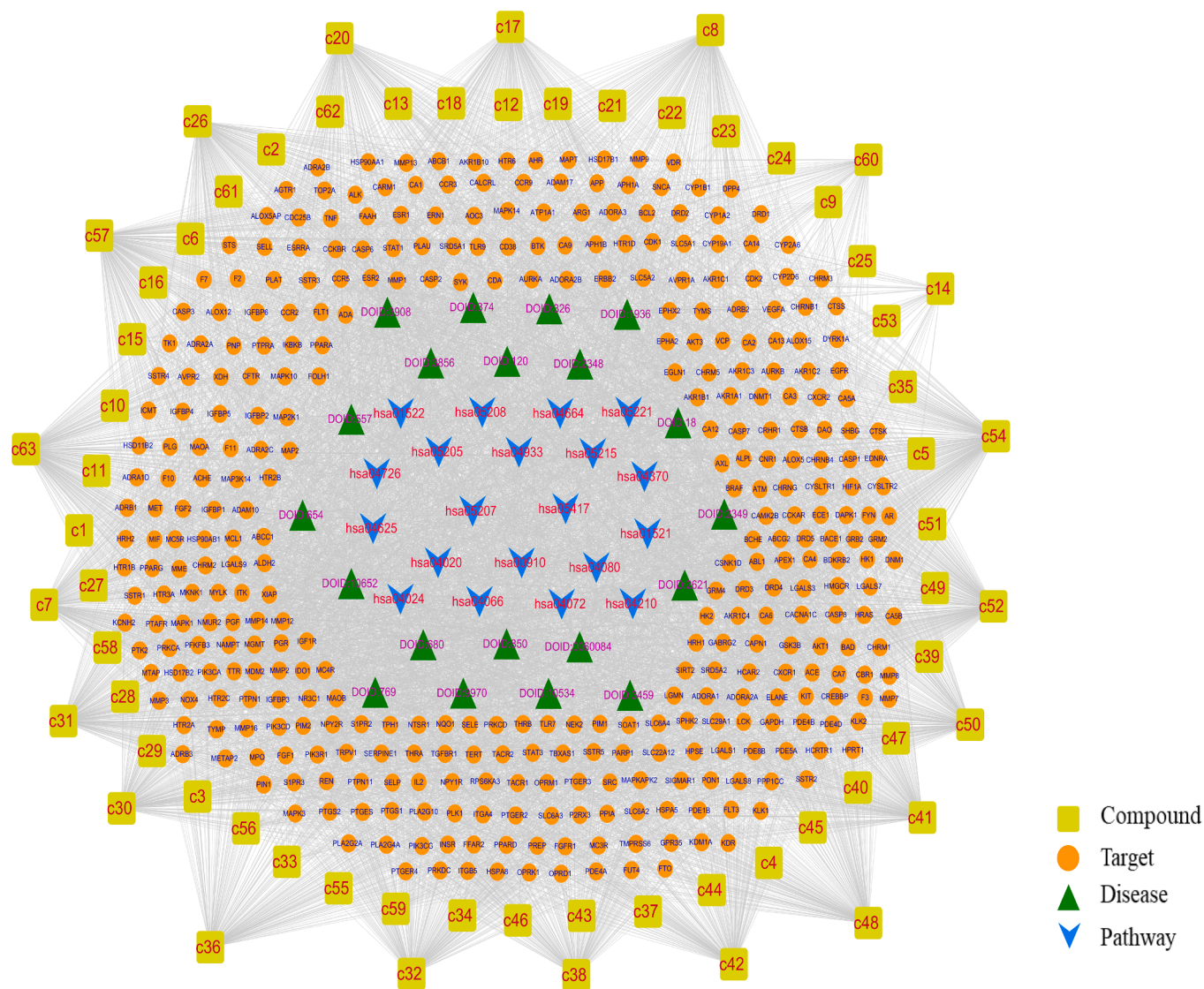


Fig. 5. The compound-target-pathway-disease network of *Rhodiola* species.

3.3. Quantitative analysis of active components

The applicability and performance of the proposed method in the determination of active components were validated, including linearity, intra-day precision, inter-day precision, LOD, LOQ, repeatability, stability, and accuracy. The results are shown in Table 1 and Table 2.

The LOD and LOQ of the 12 active components ranged from 0.957 to 4.225 ng/mL and from 3.189 to 14.085 ng/mL, respectively. And the 12

index components exhibited a satisfactory linear relationship within the concentration range of 5–1000 ng/mL. The instrument exhibited good precision, with high repeatability in the method used. Additionally, the sample solution remained stable at room temperature for 24 h. The relative standard deviation (RSD) values of accuracy, repeatability, and stability were all less than 5.50%. The sample recovery rate ranged from 98.78% to 103.35%, with RSD values consistently less than 3.30%. These results demonstrated the acceptable recovery rates of the 12

Table 1
Linear equation, linear range, LOD and LOQ of 12 compounds by UHPLC-QQQ-MS/MS analysis.

Compounds	Regression equation	r ²	Linearity range (ng/mL)	LOD (ng/mL)	LOQ (ng/mL)
Salidroside	y = 51.431x + 239.45	r ² = 0.9992	15.625–1000	3.896	12.987
Epicatechin gallate	y = 2000.8x + 1601.8	r ² = 0.9995	15.625–1000	4.225	14.085
Catechin gallate	y = 2325.2x + 6987.5	r ² = 0.9995	15.625–1000	2.871	9.569
Rhodosin	y = 5 606.3x – 4969.7	r ² = 0.9990	5–320	1.063	3.546
Luteolin	y = 8933.9x – 35,347	r ² = 0.9993	5–320	1.373	4.577
Epicatechin	y = 5334x – 4450.1	r ² = 0.9993	5–320	1.361	4.535
Isoquercitrin	y = 2637x – 2287.9	r ² = 0.9999	5–320	1.422	4.739
Afzelin	y = 1606x + 1380.3	r ² = 0.9995	5–320	1.313	4.377
Nicotiflorin	y = 1199.9x – 2797.3	r ² = 0.9997	5–320	1.325	4.415
Catechin	y = 922.28x + 13830	r ² = 0.9994	5–320	1.25	4.167
6'-O-Galloylsalidroside	y = 320.95x – 557.53	r ² = 0.9994	5–320	1.188	3.960
Eriodictyol	y = 7232.2x + 312.96	r ² = 0.9992	5–320	0.957	3.189

Table 2

The results of method validation of UHPLC-QQQ-MS/MS analysis.

Compounds	Precision RSD (%)						Repeatability RSD (%) (n = 6)	Stability RSD (%) (n = 6)	Recovery (n = 6)	
	Intra-day (n = 6)			Inter-day (n = 3)					Mean	RSD (%)
	LQC	MQC	HQC	LQC	MQC	HQC				
Salidroside	0.63	2.35	2.48	1.8	4.00	2.68	4.06	4.13	102.62	1.53
Epicatechin gallate	0.27	0.88	1.45	5.45	3.79	1.99	2.37	1.15	100.64	2.72
Catechin gallate	2.77	0.41	0.20	5.10	3.71	2.04	1.88	1.33	99.92	3.04
Rhodosin	0.80	1.07	0.58	3.14	3.46	2.63	1.65	2.16	98.78	3.13
Luteolin	1.39	1.44	1.10	3.23	3.55	4.66	1.44	2.82	99.85	2.95
Epicatechin	0.81	0.72	0.21	1.42	1.72	2.11	1.63	2.80	101.12	3.24
Isoquercitrin	0.83	1.22	0.49	0.86	1.31	0.52	1.95	1.74	103.14	1.70
Afzelin	0.59	1.48	0.29	1.33	1.70	1.00	1.84	1.66	100.37	2.49
Nicotiflorin	1.70	0.75	1.68	2.84	3.85	4.69	3.64	4.31	100.85	3.07
Catechin	0.42	1.16	0.99	1.99	1.44	3.88	3.33	2.43	102.55	2.15
6'-O-Galloylsalidroside	0.69	2.88	2.82	2.09	3.07	3.11	3.41	3.00	103.35	1.31
Eriodictyol	0.66	0.5	0.99	0.84	2.75	3.59	1.69	3.00	102.29	1.49

compounds in 9 species of *Rhodiola*, as well as the adequate accuracy and reliability of the established method.

Multiple reaction monitoring (MRM) is a highly specific and sensitive mass spectrometry technique used to quantify predefined compounds of interest. The UHPLC-MS/MS analytical method previously reported was then used to simultaneously quantify the 12 active components found in 9 species of *Rhodiola*. In order to determine the average contents of the constituents, each sample was analyzed in three separate tests. The results can be seen in Fig. 6 and Table S6.

In the disease modules of the circulatory system, the mouth and the respiratory system, the contents of luteolin were relatively high in *R. crenulata* and *R. kirilowii*, the contents of epicatechin gallate and catechin gallate were high in *R. crenulata* and *R. sacra*, and the contents of isoquercitrin and afzelin were high in *R. crenulata*. In the disease modules of the skin and the connective tissue, the contents of epicatechin gallate and catechin gallate were relatively high in *R. crenulata*, *R. sacra*, the contents of luteolin were high in *R. crenulata* and *R. kirilowii*, and the contents of isoquercitrin and afzelin were high in *R. crenulata*. In addition, from the perspective of other active components, the content of salidroside in *R. kirilowii* was equal to that of *R. crenulata*. High contents of rhodosin were determined in *R. crenulata* and *R. sacra*. The content of 6'-O-galloylsalidroside was extremely high in *R. sacra*. Finally, these findings revealed that salidroside, rhodosin,

epicatechin gallate, catechin gallate, and 6'-O-galloylsalidroside served as potential quality markers for 9 species of *Rhodiola*. *R. kirilowii* and *R. sacra* could be used as alternative species of *R. crenulata*.

4. Discussion

Traditionally, for plants with unknown pharmacological activities, the traditional approach is isolating natural products from the plant firstly, and then investigating their pharmacological activities. However, this method is both time-consuming and specificity-lacking (Aravinda et al., 2023; Royani et al., 2023). In this study, an integrated analytical method based on chemical profiling, disease module-guided network pharmacology, and quantitative analysis (CDMQ) was developed. This method provided a rapid identification of chemical composition, discovery of active components, prediction of disease module, and systematic exploration of potential quality markers to select alternative species of *R. crenulata*. It overcame the challenge of finding alternative species solely based on chemical composition or pharmacological activity. On the other hand, it provided valuable insights for the development and utilization of unknown plants, enabling the rapid discovery of pharmacological activities and potential quality markers.

Different species of plants in the same genus have varying pharmacological activities due to differences in chemical composition. It has

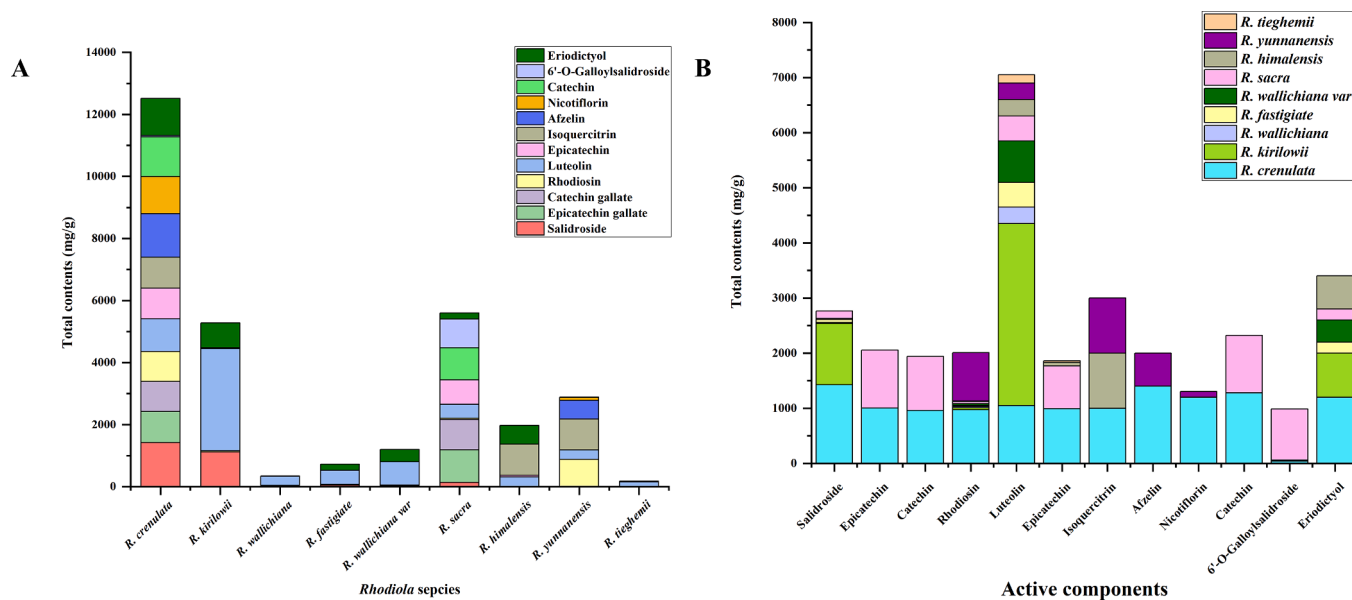


Fig. 6. Determination of the contents of 12 active compounds. A: Comparison of the total contents among *Rhodiola* species. B: Comparison of the content of individual compound among *Rhodiola* species.

been found that *R. crenulata* showed a high content of phenolic acids with significant antioxidant activity compared to that of *Rhodiola rosea* (Dong et al., 2021). BooKer assessed the quality of *R. crenulata* and *Rhodiola rosea* by analyzing the difference in their phytochemical composition (BooKer et al., 2016). Studying the material basis of drug action are often limited by the challenge of determining the chemical composition of single plant (Cheng et al., 2022; Li et al., 2023a, 2023b, 2023d). In the present study, the chemical compositions of 9 species of *Rhodiola* were characterized, and the results showed that *R. crenulata* with a more abundant chemical composition compared to other species. Additionally, significant differences in chemical composition were observed among 9 species of *Rhodiola*. The comprehensive identification of chemical components across multiple species of *Rhodiola* had therefore laid a solid foundation for the exploration of disease module-guided network pharmacology.

Generally, network pharmacology studies utilize public databases to gather information about the components of Chinese medicine (Tao et al., 2023; Chen et al., 2023). However, there are significant differences in the chemical composition of Chinese medicine derived from different species, which can greatly impact their pharmacological activities (Tao et al., 2019; Shikov et al., 2021; Panossian et al., 2021). Furthermore, more attention has traditionally been paid to the identification of chemical composition of individual species of Chinese medicine (Chen et al., 2022b; Ning et al., 2022; Yang et al., 2021). Instead of relying on databases and single-species plant studies, this study fully characterized the chemical compositions of 9 species of *Rhodiola*. The characteristics of “multi-component, multi-target, and multi-pathway” determine that traditional Chinese medicine do not only act on single disease (Dong et al., 2024; Liu et al., 2023). However, traditional network pharmacology studies often focus on a specific disease of Chinese medicine, which significantly restricts the development of pharmacodynamic research of Chinese medicine (Li et al., 2023b, 2023c, 2023d; Zhang et al., 2024). In this study, a comprehensive chemical identification of 9 species of *Rhodiola* was performed, instead of relying on traditional chemical composition databases and single species chemical composition identifications. Then, in order to break the barrier of traditional network pharmacology (Li et al., 2023b, 2023c, 2023d; Sun et al., 2023), a disease module-guided approach was performed. According to the ICD-11, the concept of disease module was introduced and disease module - active component network diagram was constructed. The top 10 diseases were divided into 5 disease modules, including the circulatory system, the skin, the connective tissue, the mouth, and the respiratory system. Through the compound-target-pathway-disease network analysis, 12 active components were selected. Salidroside, as the primary active component in *Rhodiola*, possesses various pharmacological activities, including anti-hypoxia, anti-fatigue, protection of nerve cells, cardiovascular and cerebrovascular protection, anti-acute lung injury, and anti-atherosclerosis effects. Salidroside can simultaneously decrease de novo lipogenesis and cholesterol biosynthesis, which contribute to the attenuation of atherosclerosis in mice (Song et al., 2021). Salidroside has been shown to improve endothelial function and alleviate atherosclerosis by activating the AMPK/PI3K/Akt/eNOS pathway in mitochondria (Xing et al., 2015). Meanwhile, bioactivities of the other compounds were also supported by previous literatures (Cao et al., 2022; Chen et al., 2022c; Jin et al., 2023; Li et al., 2023a). In addition, the 75% ethanol extract of *R. wallichiana* var (RW) showed cardioprotective effects on H9c2 cells and I/R injury in rats by attenuating oxidative stress-mediated apoptosis through enhancing Nrf2 signaling (Yan et al., 2023). The 70% ethanol extract of *R. fastigiata* has been demonstrated with significant antioxidant activity. Besides salidroside, our study also found other active components such as luteolin, epicatechin gallate, catechin gallate, afzelin, isoquercitrin, and rhodiosin, which played a crucial role in different disease modules.

The development of alternative species in traditional Chinese medicine is a complex and long-standing issue that requires careful

consideration and solutions. Because of the complexity of the chemical components of traditional Chinese medicine, it is not feasible to search alternative species for traditional Chinese medicine (Li et al., 2023a; Sun et al., 2022a, 2022b). Even though *R. crenulata* has traditionally been used as a herbal medicine, multiple experiments have focused on the effects of salidroside. Other active components in *R. crenulata* have rarely been studied (Jin et al., 2023; Calabrese et al., 2023). The UPLC/QQQ-MS/MS technology equipped with electrospray ionization was used to establish a method for the simultaneous detection of multiple active components in the 9 species of *Rhodiola* to evaluate alternative species for *R. crenulata*. In combination with disease module-guided network pharmacology, salidroside, rhodiosin, epicatechin gallate, catechin gallate, and 6'-*O*-galloylsalidroside served as potential quality markers for *Rhodiola* species and *R. kirilowii* and *R. sacra* were probably used as alternative species of *R. crenulata*.

5. Conclusion

In this study, an integrated strategy based on chemical profiling, disease module-guided network pharmacology, and quantitative analysis (CDMQ) was developed. Our approach aimed to quickly identify chemical compositions and choose potential quality markers to evaluate alternative species for *R. crenulata* in a step-by-step manner. A total of 109 compounds were identified, 12 active compounds were subsequently selected based on the disease module-guided network pharmacology analysis. Furthermore, the contents of 12 compounds were determined in the 9 species of *Rhodiola*. Through examining the content distributions of active components in the *Rhodiola* extracts, the species which were good at regulating each disease module were identified. Finally, *R. kirilowii* and *R. sacra* were chosen as the alternative species of *R. crenulata* based on the quality markers. This study offers theoretical references for the clinical application and quality control research of 9 species of *Rhodiola*. It also provides suggestions for the development of alternative species to *R. crenulata*.

Declaration of Competing Interest

The authors declare that they have no known competing financial interests or personal relationships that could have appeared to influence the work reported in this paper.

Acknowledgements

This study was supported by the Tianjin Committee of Science and Technology of China (No. 23ZYJDS00030) and the Science and Technology Project of Haihe Laboratory of Modern Chinese Medicine (Nos. 22HHZYSS00007 and 22HHZYJC00003).

Appendix A. Supplementary data

Supplementary data to this article can be found online at <https://doi.org/10.1016/j.arabjc.2023.105570>.

References

- Aravinda, H., Shivakumara, K.T., Chandrashekhara, K., Rani, A.T., Casini, R., Sayed, S.R., Elansary, H.O., El-Sabrou, A.M., 2023. Isolation of antimicrobial peptides from seed harvester ant, *Trichomyrmex scabriceps* (Mayr) (Hymenoptera: Formicidae) and their antimicrobial assay. *Arab. J. Chem.* 16 (10) <https://doi.org/10.1016/j.arabjc.2023.105162>.
- Booker, A., Zhai, L.X., Gkouva, C., Li, S.Y., Heinrich, M., 2016. From traditional resource to global commodities: —a comparison of *Rhodiola* species using NMR spectroscopy—metabolomics and HPTLC. *Front. Pharmacol.* 7 <https://doi.org/10.3389/fphar.2016.00254>.
- Calabrese, E.J., Dhawan, G., Kapoor, R., Agathokleous, E., Calabrese, V., 2023. *Rhodiola rosea* and salidroside commonly induce hormesis, with particular focus on longevity and neuroprotection. *Chem Biol Interact.* 380, 110540 <https://doi.org/10.1016/j.cbi.2023.110540>.

- Cao, L., Lin, H., Li, Q., Han, S.Z., Yin, H., Zhang, N., Gao, Y.F., Chen, Y., Ping, F., 2022. Study on lung injury caused by fine particulate matter and intervention effect of *Rhodiola wallichiana*. *Evid Based Compl. Alternat. Med.* 2022, 3693231. <https://doi.org/10.1155/2022.3693231>.
- Chen, F., Chai, Y.H., Zhang, F., Liu, Y.Q., Zhang, Y., Shi, Y.J., Zhang, J.M., Leng, Y.F., 2023. Network pharmacology analysis combined with experimental validation to explore the therapeutic mechanism of salidroside on intestine ischemia reperfusion. *Biosci. Rep.* 43 (8) <https://doi.org/10.1042/BSR20230539>. BSR20230539.
- Chen, Y., Tang, M., Yuan, S., Fu, S., Li, Y.F., Li, Y., Wang, Q., Cao, Y., Liu, L., Zhang, Q., 2022a. *Rhodiola rosea*: a therapeutic candidate on cardiovascular diseases. *Oxid. Med. Cell Longev.* 1348795 <https://doi.org/10.1155/2022/1348795>.
- Chen, T.T., Wang, X.N., Chen, P., Zheng, Y.Y., He, Y., Zeng, X., Peng, W., Su, W.W., 2022b. Chemical components analysis and in vivo metabolite profiling of *Jian'er Xiaoshi oral liquid* by UHPLC-Q-TOF-MS/MS. *J. Pharm. Biomed. Ana.* 211, 114629 <https://doi.org/10.1016/j.jpba.2022.114629>.
- Chen, H., Zhu, J., Le, Y.F., Pan, J.L., Liu, Y., Wang, C., Dou, X.B., Lu, D.Z., 2022c. Salidroside inhibits doxorubicin-induced cardiomyopathy by modulating a ferroptosis-dependent pathway. *Phytomedicine* 99, 153964. <https://doi.org/10.1016/j.phymed.2022.153964>.
- Cheng, X., Li, B.P., Han, Z.X., Zhang, F.L., Jiang, Z.R., Yang, J.S., Luo, Q.Z., Tang, L., 2022. Qualitative and quantitative analysis of the major components in *Qinghao Biejia decoction* by UPLC-Orbitrap Fusion-MS/MS and UPLC-QQ-MS/MS and evaluation of their antibacterial activities. *Phytochem. Anal.* 33 (5), 809–825. <https://doi.org/10.1002/pca.3131>.
- Chinese Pharmacopoeia Commission, 2020. *Pharmacopoeia of the People's Republic of China*. China Medical Science Press, Beijing, p. 161.
- Choe, K.I., Kwon, J.H., Park, K.H., Oh, M.H., Kim, M.H., Kim, H.H., Cho, S.H., Chung, E. K., Ha, S.Y., Lee, M.W., 2012. The antioxidant and anti-inflammatory effects of phenolic compounds isolated from the root of *Rhodiola sachalinensis* A. BOR. *Molec.* 17 (10), 11484–11494. <https://doi.org/10.3390/molecules171011484>.
- Chu, Y.H., Wu, H., Hsieh, J.F., 2014. Isolation and characterization of α -glucosidase inhibitory constituents from *Rhodiola crenulata*. *Food Res Int.* 57, 8–14. <https://doi.org/10.1016/j.foodres.2014.01.029>.
- Coudert, E., Gehant, S., de Castro, E.D., Pozzato, M., Baratin, D., Neto, T., Sigrist, C.J.A., Redaschi, N., Bridge, A., 2023. Annotation of biologically relevant ligands in UniProtKB using ChEBI. *Bioinformatics*. 39 (1), btac793. <https://doi.org/10.1093/bioinformatics/btac793>.
- Diermen, D.V., Marston, A., Bravo, J., Reist, M., Carrupt, P.A., Hostettmann, K., 2009. Monoamine oxidase inhibition by *Rhodiola rosea* L. roots. *J. Ethnopharmacol.* 122 (2), 397–401. <https://doi.org/10.1016/j.jep.2009.01.007>.
- Dong, T., Liu, H., Sha, Y., Sun, L., 2023. A comparative study of phytochemical metabolites and antioxidant properties of *Rhodiola*. *Arab. J. Chem.* 16 (1), 104420 <https://doi.org/10.1016/j.arabj.2022.104420>.
- Dong, T.T., Sha, Y.Q., Liu, H.R., Sun, L.W., 2021. Altitudinal variation of metabolites, mineral elements and antioxidant activities of *Rhodiola crenulata* (Hook.f. & Thomson) H. Ohba. *Molecules* 26 (23), 7383. <https://doi.org/10.3390/molecules26237383>.
- Dong, B.H., Wu, J., Peng, Y., Jiang, Y.X., Cao, M.Y., Huang, Y., Hu, C.J., Yu, L.Y., Chen, Z.M., 2024. A multi-strategy platform for Q-markers screening and quality control of *Wuzi Yanzong Wan* based on fingerprint and network pharmacology. *Arab. J. Chem.* 17 (1), 105435 <https://doi.org/10.1016/j.arabj.2023.105435>.
- Döring, K., Langeder, J., Duwe, S., Tahir, A., Grienke, K., Rolling, J.M., Schmidtke, M., 2022. Insights into the direct anti-influenza virus mode of action of *Rhodiola rosea*. *Phytomedicine*. 96, 153895 <https://doi.org/10.1016/j.phymed.2021.153895>.
- Ge, B., Guo, C., Liang, Y.J., Liu, M.Z., Wu, K., 2019. Network analysis, and human and animal studies disclose the anticystitis glandularis effects of vitamin C. *Biofactors* 45 (6), 912–919. <https://doi.org/10.1002/biot.1558>.
- Grosso, C., Santos, M., Barroso, M.F., 2023. From plants to psycho-neurology: unravelling the therapeutic benefits of bioactive compounds in brain disorders. *Antioxidants* 12 (8), 1603. <https://doi.org/10.3390/antiox12081603>.
- Hopkins, A.L., 2007. Network pharmacology: the next paradigm in drug discovery.
- Hsu, S.W., Chang, T.C., Wu, Y.K., Lin, K.T., Shi, L.S., Lee, S.Y., 2017. *Rhodiola crenulata* extract counteracts the effect of hypobaric hypoxia in rat heart via redirection of the nitric oxide and arginase 1 pathway. *BMC Compl. Altern. Med.* 17 (1), 29. <https://doi.org/10.1186/s12906-016-1524-z>.
- Jafari, M., Juanson Arabit, J.G., Courville, R., Kiani, D., Chaston, J.M., Nguyen, C.D., Jena, N., Liu, Z., Tata, P., Etten, R.V., 2022. The impact of *Rhodiola rosea* on biomarkers of diabetes, inflammation, and microbiota in a leptin receptor-knockout mouse model. *Sci. Rep.* 12 (1), 10581. <https://doi.org/10.1038/s41598-022-14241-7>.
- Jia, X.H., Zhang, K., Feng, S.S., Li, Y.Y., Yao, D.H., Liu, Q.H., Liu, D., Li, X., Huang, J., Wang, H.Y., Wang, J.H., 2023. Total glycosides of *Rhodiola rosea* L. attenuate LPS-induced acute lung injury by inhibiting TLR4/NF- κ B pathwa. *Biomed. Pharmacother.* 158, 114186 <https://doi.org/10.1016/j.biopha.2022.114186>.
- Jin, T., Lian, W.S., Zhang, X.J., Wang, S.Q., Xu, M.J., Sherchan, A., Li, M.Q., 2023. An in vitro study on probable inhibition of cerebrovascular disease by salidroside as a potent small molecule against induction of protein amyloid fibrils and cytotoxicity. *Arab. J. Chem.* 16 (4), 104548 <https://doi.org/10.1016/j.arabj.2023.104548>.
- Jung, W., Lee, D., Kim, J., Choi, I., Park, S., Seo, S., Lee, S., Lee, C., Park, Y., Jeon, Y., Lee, C., Jeon, B., Qian, Z., Kim, S., Choi, I., 2008. Anti-inflammatory activity of caffeic acid phenethyl ester (CAPE) extracted from *Rhodiola sacra* against lipopolysaccharide-induced inflammatory responses in mice. *Process Biochem.* 43 (7), 783–787. <https://doi.org/10.1016/j.procbio.2008.03.004>.
- Li, X.Q., Chen, S.P., Shao, W.H., Wang, S.X., Yao, L.X., 2023a. Investigating the effects and mechanism of *Rhodiola Rosea* injection on cardiac function in rats with chronic heart failure. *Comb. Chem. High Throughput Screen.* 26 (12), 2238–2246. <https://doi.org/10.2174/1386207326666230203145254>.
- Li, M.H., Liu, J.H., La, C.W., Liu, T., Zhao, Z.B., Wang, Z., Dai, M.H., Chen, J.M., Ren, Z., Ye, C.F., Wang, Y.F., 2023b. Exploring the mechanism of *Artemisia argyi* chemical composition for ulcerative colitis based on network pharmacology. *Arab. J. Chem.* 16 (9), 105050 <https://doi.org/10.1016/j.arabj.2023.105050>.
- Li, G.T., Wang, X.R., Luo, L.F., Zhang, H., Song, X.B., Zhang, J.Z., Liu, D.L., 2023c. Identification of chemical constituents of *Qingjin Yiqi granules* and comparative study on pharmacokinetics of 23 main bioactive components in normal and Lung-Qi deficiency rats by UPLC-MS/MS method. *J. Chromatogr. B Analyt. Technol. Biomed. Life Sci.* 1226, 123802 <https://doi.org/10.1016/j.jchromb.2023.123802>.
- Li, K.L., Yao, Q., Zhang, M., Li, Q., Guo, L.L., Li, J., Yang, J.B., Cai, W., 2023d. Exploring the effective components and potential mechanisms of *Zukamu granules* against acute upper respiratory tract infections by UHPLC-Q-Exactive Orbitrap-MS and network pharmacology analysis. *Arab. J. Chem.* 16 (8), 104875 <https://doi.org/10.1016/j.arabj.2023.104875>.
- Li, S., Zhang, B., 2013. Traditional Chinese medicine network pharmacology: theory, methodology and application. *Chin. J. Nat. Med.* 11 (2), 110–120. <https://doi.org/10.3724/SP.J.1009.2013.00110>.
- Liang, T.S., Zhou, J.X., Jing, P., He, Z.J., Jiao, S.S., Zhao, W.J., Tong, Q., Jia, G.F., 2023. Anti-senescence effects of *Rhodiola crenulata* extracts on LO2 cells and bioactive compounds. *J. Ethnopharmacol.* 116179 <https://doi.org/10.1016/j.jep.2023.116179>.
- Liu, S.H., Hsiao, Y.W., Chong, E., 2016. *Rhodiola* inhibits atrial arrhythmogenesis in a heart failure model. *J. Cardiovasc. Electrophysiol.* 27 (9), 1093–1101. <https://doi.org/10.1111/jce.13026>.
- Liu, C.J., Jiang, Q.B., Zhou, Z.R., Lei, P., Chai, X., Pan, G.X., Wang, Y.F., Jiang, M.M., 2024. Studies on chemical profiling and pharmacokinetics of traditional Chinese medicine Formula *Kang Shuai Lao Pian*. *Arab. J. Chem.* 17 (1), 105398 <https://doi.org/10.1016/j.arabj.2023.105398>.
- Liu, L.X., Li, H.B., Zhang, J.Y., Shi, D.F., Wang, Z.Z., Yao, X.S., Xiao, W., Yu, Y., 2023. Quality markers screening of traditional Chinese medicine prescriptions based on the multi-factor analysis strategy: Jin-Zhen Oral Liquid as a case. *Arab. J. Chem.* 105433 <https://doi.org/10.1016/j.arabj.2023.105433>.
- Ma, Y.G., Wang, J.W., Bai, Y.G., Liu, M., Xie, M.J., Dai, Z.J., 2017. Salidroside contributes to reducing blood pressure and alleviating cerebrovascular contractile activity in diabetic Goto-Kakizaki Rats by inhibition of L-type calcium channel in smooth muscle cells. *BMC Pharmacol. Toxicol.* 18 (1), 30. <https://doi.org/10.1186/s40360-017-0135-8>.
- Ma, D.D., Wang, L.J., Jin, Y.B., Gu, L.F., Yin, G., Wang, J., Yu, X.A., Huang, H.S., Zhang, Z., Wang, B., Lu, Y., Bi, K.S., Wang, P., Wang, T.J., 2022. Chemical characteristics of *Rhodiola crenulata* and its mechanism in acute mountain sickness using UHPLC-Q-TOF-MS/MS combined with network pharmacology analysis. *J. Ethnopharmacol.* 294, 115345 <https://doi.org/10.1016/j.jep.2022.115345>.
- Mendez, D., Gaulton, A., Bento, A.P., Chambers, J., De Veij, M., Félix, E., Magariños, M. P., Mosquera, J.F., 2019. ChEMBL: towards direct deposition of bioassay data. *Nucl. Acids Res.* 47 (D1), D930–D940. <https://doi.org/10.1093/nar/gky1075>.
- Ning, J.R., Wang, K.H., Yang, W.L., Liu, M.S., Tian, J.Y., Wei, M.Y., Zheng, G.D., 2022. Qualitative and quantitative analyses of chemical components of *Citri Sarcodactylis* Fructus from different origins based on UPLC-Q-Exactive Orbitrap-MS and GC-MS. *Food Sci. Nutr.* 10 (6), 2057–2070. <https://doi.org/10.1002/fsn3.2822>.
- Panossian, A.G., Efferth, T., Shikov, A.N., Pozharitskaya, O.N., Kuchta, K., Mukherjee, P. K., Banerjee, S., Heinrich, M., Wu, W., Guo, D.A., Wagner, H., 2021. Evolution of the adaptogenic concept from traditional use to medical systems: pharmacology of stress- and aging-related diseases. *Med. Res. Rev.* 41 (1), 630–703. <https://doi.org/10.1002/mrd.21743>.
- Parham, S., Kharazi, A.Z., Bakhsheshi-Rad, H.Z., Nur, H., Ismail, A.F., Sharif, S., RamaKrishna, S., Berto, F., 2020. Antioxidant, antimicrobial and antiviral properties of herbal materials. *Antioxidants*. 9 (12), 1309. <https://doi.org/10.3390/antiox9121309>.
- Park, M., Park, S.Y., Lee, H.J., Kim, C.E., 2018. A systems-level analysis of mechanisms of *Platycodon grandiflorum* based on a network pharmacological approach. *Molecules* 23 (11), 2841. <https://doi.org/10.3390/molecules23112841>.
- Ren, J.N., Wang, R.R., Fan, W.J., Li, T., Dong, P.Z., Pan, G.X., Ren, M., Jiang, M.M., 2022. Qualitative and quantitative analysis of multi-components in *Xing-Su-Ning Capsules* for quality improvement. *Arab. J. Chem.* 15 (6), 103825 <https://doi.org/10.1016/j.arabj.2022.103825>.
- Royani, A., Hanafi, M.N., Lotulung, P.D., Prastya, M.E., Verma, C., Manaf, A., Alfantazi, A., 2023. Isolation and identification of bioactive compounds from *Tinospora cordifolia* stem extracts as antibacterial materials in seawater environments. *Arab. J. Chem.* 16 (9) <https://doi.org/10.1016/j.arabj.2023.105014>.
- Shen, W.T., Song, Z.G., Zhong, X., Huang, M., Shen, D.T., Gao, P.P., Qian, X.Q., Wang, M. M., He, X.B., Wang, T.L., Li, S., Song, X., 2022. Sangerbox: a comprehensive, interaction-friendly clinical bioinformatics analysis platform. *iMeta* 1 (3), e36.
- Shikov, A.N., Narkevich, I.A., Flisyuk, E.V., Luzhanin, V.G., Pozharitskaya, O.N., 2021. Medicinal plants from the 14th edition of the Russian Pharmacopoeia, recent updates. *J. Ethnopharmacol.* 268 <https://doi.org/10.1016/j.jep.2020.113685>.
- Song, T.X., Wang, P.L., Li, C.Y., Jia, L., Liang, Q.Q., Cao, Y.L., Dong, P.Z., Shi, H., Jiang, M.M., 2021. Salidroside simultaneously reduces de novo lipogenesis and cholesterol biosynthesis to attenuate atherosclerosis in mice. *Biomed. Pharmacother.* 134, 111137 <https://doi.org/10.1016/j.biopha.2020.111137>.
- Sun, F.F., Liu, J.D., Xu, J.F., Tariq, A., Wu, Y.N., Li, L., 2023. Molecular mechanism of Yi-Qi-Yang-Yin-Ye against obesity in rats using network pharmacology, molecular docking, and molecular dynamics simulations. *Arab. J. Chem.* 17 (1), 105390 <https://doi.org/10.1016/j.arabj.2023.105390>.

- Sun, S.T., Wang, M.S., Yuan, Y., Wang, S., Ding, H.R., Liang, C.R., Li, X.M., Fan, S.M., Li, Y.B., 2022a. A new strategy for the rapid identification and validation of direct toxicity targets of psoralen-induced hepatotoxicity. *Toxicol. Lett.* 363, 11–26. <https://doi.org/10.1016/j.toxlet.2022.05.002>.
- Sun, P., Zhao, W.J., Wang, Q., Chen, L.L., Sun, K.K., Zhan, Z.S., Wang, J.F., 2022b. Chemical diversity, biological activities and Traditional uses of and important Chinese herb Sophora. *Phytotherap. J.* 100, 154054 <https://doi.org/10.1016/j.phymed.2022.154054>.
- Tao, L., Liang, Z.F., Miao, L., Guo, Y.J., Li, Y., Liu, Y.L., Fang, D.M., Yang, Z.J., 2023. Mechanism of salidroside against coronary artery disease by network pharmacology analysis. *BMC Compl. Med. Ther.* 23 (1), 194. <https://doi.org/10.1186/s12906-023-04027-3>.
- Tao, H.X., Wu, X., Cao, J.L., Peng, Y., Wang, A.Q., Pei, J., Xiao, J.B., Wang, S.P., Wang, Y. T., 2019. *Rhodiola* species: a comprehensive review of traditional use, phytochemistry, pharmacology, toxicity, and clinical study. *Med. Res. Rev.* 39 (5), 1779–1850. <https://doi.org/10.1002/med.21564>.
- Teng, S.G., Qian, X., Zheng, J.H., Qian, J., 2022. The efficacy and safety of *Rhodiola* formulation for the treatment of ischemic heart disease: a protocol for systematic review and meta-analysis. *Medicine (Baltimore)* 101 (45), e31736.
- Wang, J.Y., Xie, N., Li, M.J., Su, J.S., Hou, Y., Zhang, Y., Wang, X.B., 2023. Field collection and laboratory routine identification of *Rhodiola crenulata*. *J. Vis. Exp.* 200 <https://doi.org/10.3791/65947>.
- Wen, J., Lv, X.M., Hong, D.X., Xie, C.X., Zhang, J., Zhang, Y., 2016. Potential distribution of *Rhodiola crenulata* in Tibetan Plateau based on Maxent model. *Zhongguo Zhong Yao Za Zhi* 41 (21), 3931–3936. <https://doi.org/10.4268/cjcm20162108>.
- Wojcik, R., Siwicki, A., Rózewicka, E.S., Wasutyński, A., 2009. The effect of Chinese medicinal herb *Rhodiola kirilowii* extracts on cellular immunity in mice and rats. *Pol. J. Vet. Sci.* 12 (3), 399–405.
- Xing, S.S., Yang, X.Y., Zheng, T., Li, W.J., Wu, D., Chi, J.Y., Bian, F., Bai, X.L., Wu, G.J., Zhang, Y.Z., Zhang, C.T., Zhang, Y.H., Li, Y.S., Jin, S., 2015. Salidroside improves endothelial function and alleviates atherosclerosis by activating a mitochondria-related AMPK/PI3K/Akt/eNOS pathway. *Vascul. Pharmacol.* 72, 141–152. <https://doi.org/10.1016/j.vph.2015.07.004>.
- Xu, H.Y., Zhang, Y.Q., Liu, Z.M., Chen, T., Lv, C.Y., Tang, S.H., Zhang, X.B., Zhang, W., Li, Z.Y., Zhou, R.R., Yang, H.J., Wang, X.J., Huang, L.Q., 2018. ETCM: an encyclopaedia of traditional Chinese medicine. *Nucl. Acids Res.* 47 (D1), D976–D982. <https://doi.org/10.1093/nar/gky987>.
- Yan, T., Li, X., Wang, X., Zhang, Y., He, B., Jia, Y., Xiao, W., 2023. *Rhodiola wallichiana* var. *cholaensis* protects against myocardial ischemia-reperfusion injury by attenuating oxidative stress-mediated apoptosis via enhancing Nrf2 signaling. *Int. J. Cardiol.* 384, 62–73. <https://doi.org/10.1016/j.ijcard.2023.05.014>.
- Yang, S.S., Zhang, X.Y., Dong, Y.Q., Sun, G.J., Jiang, A.L., Li, Y.B., 2021. Cleavage rules of mass spectrometry fragments and rapid identification of chemical components of *Radix Paoniae Alba* using UHPLC-Q-TOF-MS. *Phytochem. Anal.* 32 (5), 836–849. <https://doi.org/10.1002/pca.3029>.
- Ye, X.W., Deng, Y.L., Xia, L.T., Ren, H.M., Zhang, J.L., 2020. Uncovering the mechanism of the effects of *Paoniae Radix Alba* on iron-deficiency anaemia through a network pharmacology-based strategy. *BMC Compl. Med. Ther.* 20 (1), 130. <https://doi.org/10.1186/s12906-020-02925-4>.
- Zhang, X., Huang, Y., Yang, Z.T., Xu, B.Y., Liu, Z.L., Ding, X.M., Zhou, Q.M., Cao, G., Li, W.D., Jin, C.S., Li, S.S., Wang, X.L., Chu, J.J., 2024. Exploring the mechanism of *Semen Cuscutae* processed with salt solution in improving kidney deficiency miscarriage based on serum pharmacochemistry and network pharmacology. *Arab. J. Chem.* 17 (1), 105456 <https://doi.org/10.1016/j.arabjc.2023.105456>.
- Zhang, B., Li, Q.Q., Chu, X.K., Sun, S.Y., Chen, S.D., 2016. Salidroside reduces tau hyperphosphorylation via up-regulating GSK-3 β phosphorylation in a tau transgenic Drosophila model of Alzheimer's disease. *Transl. Neurodegener.* 5, 21. <https://doi.org/10.1186/s40035-016-0068-y>.
- Zhao, C.Y., Jia, G.F., He, Z.J., Luo, Q.F., Fan, G., Zhang, Y., Zhao, W.J., 2018. Effect of fertilization combinations of nitrogen, phosphorus, and potassium on four phenolic compounds of cultivated *Rhodiola crenulata*. *Zhongguo Zhong Yao Za Zhi* 43 (9), 1812–1817. <https://doi.org/10.19540/j.cnki.cjcm.20180201.013>.
- Zheng, T., Bian, F., Chen, L., Wang, Q.B., Jin, S., 2019. Beneficial effects of *Rhodiola* and Salidroside in diabetes: potential role of AMP-activated protein kinase. *Mol. Diagn. Ther.* 23 (4), 489–498. <https://doi.org/10.1007/s40291-019-00402-4>.
- Zhong, D.L., Li, Y.C., Zhang, J.Q., 2022. Allopolyploid origin and niche expansion of *Rhodiola integrifolia* (Crassulaceae). *Plant Divers.* 45 (1), 36–44. <https://doi.org/10.1016/j.pld.2022.08.004>.
- Zhuang, W., Yue, L.F., Dang, X.F., Chen, F., Gong, Y.W., Lin, X.L., Luo, Y.M., 2019. Rosenroot (*Rhodiola*): potential applications in aging-related diseases. *Aging Dis.* 10 (1), 134–146. <https://doi.org/10.14336/AD.2018.0511>.